Supporting Information

On-resonance Fluorescence, Resonance Rayleigh Scattering, and Ratiometric Resonance Synchronous Spectroscopy of Molecular- and Quantum Dot-Fluorophores

Kumudu Siriwardana,[†] Charles B. Nettles II,[†] Buddhini C.N. Vithanage,[†] Yadong Zhou,[§] Shengli Zou,[§,] and Dongmao Zhang[†,*]*

† Department of Chemistry, Mississippi State University, Mississippi State, Mississippi 39762, United States

§ Department of Chemistry, University of Central Florida, Orlando, Florida 32816, United States

[*]*Corresponding author: Email: Dongmao@chemistry.msstate.edu, Shengli.zou@ucf.edu*

Fax: 662-325-1618 (Zhang), 407-823-2252 (Zou)

Contents **Page**

S1. Materials and Instruments

All molecular fluorophores, organic solvents, and the toluene-soluble QDs (product #753823-1KT, λ_{em} 490-665 nm) were purchased from Sigma-Aldrich and used as received. The water-soluble QD617 (product # CZW-0-1) was acquired from NN-Labs Nanopure water (18 MΩ cm) was used in aqueous solution preparation. All UV-vis spectra were acquired using a Thermo Scientific Evolution 300 UV-vis spectrophotometer with 1 nm resolution. The resonance synchronous and Stokes-shifted fluorescence spectra were acquired using a Horiba Jobin Yvon fluoromax-4-spectrofluorometer. The diameter of the water-soluble quantum dot (QD617) was 10 nm and all the toluene-soluble QDs were 6 nm in diameter.

S2. Excitation wavelength and emission wavelength ranges of the fluorophores

Table S1. Excitation and emission wavelengths of fluorophores.

Fluorophore	Excitation wavelength (nm)	Emission wavelength range (nm)
QD490	240 410	250-440 420-800
QD525	240 450	250-440 460-800
QD575	290 490	300-520 500-800
QD630	320 560	350-410 570-800
QD665	320 580	350-610 590-800
QD617	320 400	350-610 410-800
ANT	290 450	300-490 460-800
DPT	290 490	300-500 500-800
AOH	280 490	290-510 500-800
R6G	290 500	300-530 510-800
FITC	215 400	220-420 405-795
ZPC	290 410	300-450 420-800
CVP	290 500	300-550 510-800
Harmane	290 500	300-550 510-800
Harmine	290 540	300-550 550-800
Norharmane	290 530	300-550 540-800
DPA	290 530	300-550 540-800
Eosin Y	290 450	300-480 460-800

S3. Experimental data obtained with molecular fluorophore 3,3'-dipropylthiadicarbocyanine iodine (DPT)

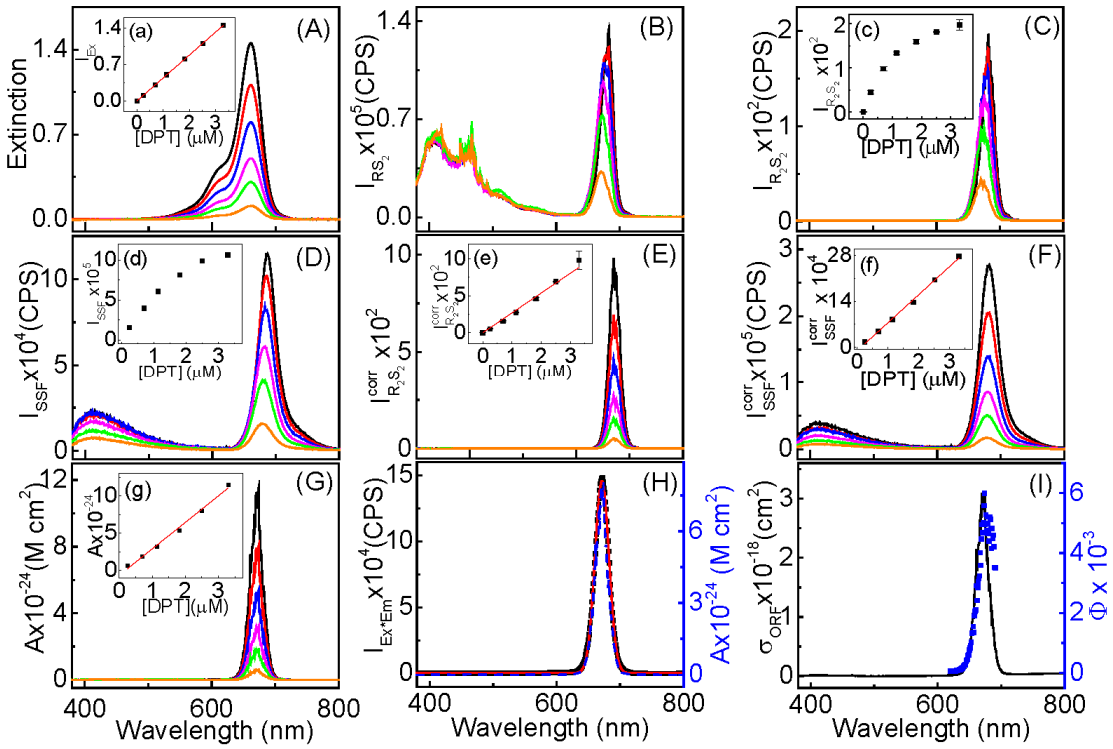

Figure S1. Experimental data obtained with molecular fluorophore DPT. Concentration-dependent (A) fluorophore UV-vis extinction spectra, (B) as-acquired RS_2 spectra, (C) as-acquired R_2S_2 spectra, (D) as-acquired SSF spectra, (E) IFE-corrected R_2S_2 spectra, (F) IFE-corrected SSF spectra, (G) R_2S_2 activity spectra, (H) Comparison of a representative (dash blue line) ORF activity spectrum, (black dots) the multiplication product spectrum of UV-vis excitation and emission spectrum, and (solid red line) the Gaussian curve fitted spectrum. (I) (Black line) ORF cross-section and (blue square) quantum yield as a function of wavelength. The inset in plots (A), (C), (D), (E), (F), and (G) are spectral peak intensity as DPT concentration.

S4. Experimental data obtained with molecular fluorophore acridine orange hemi(zinc chloride) salt (AOH)

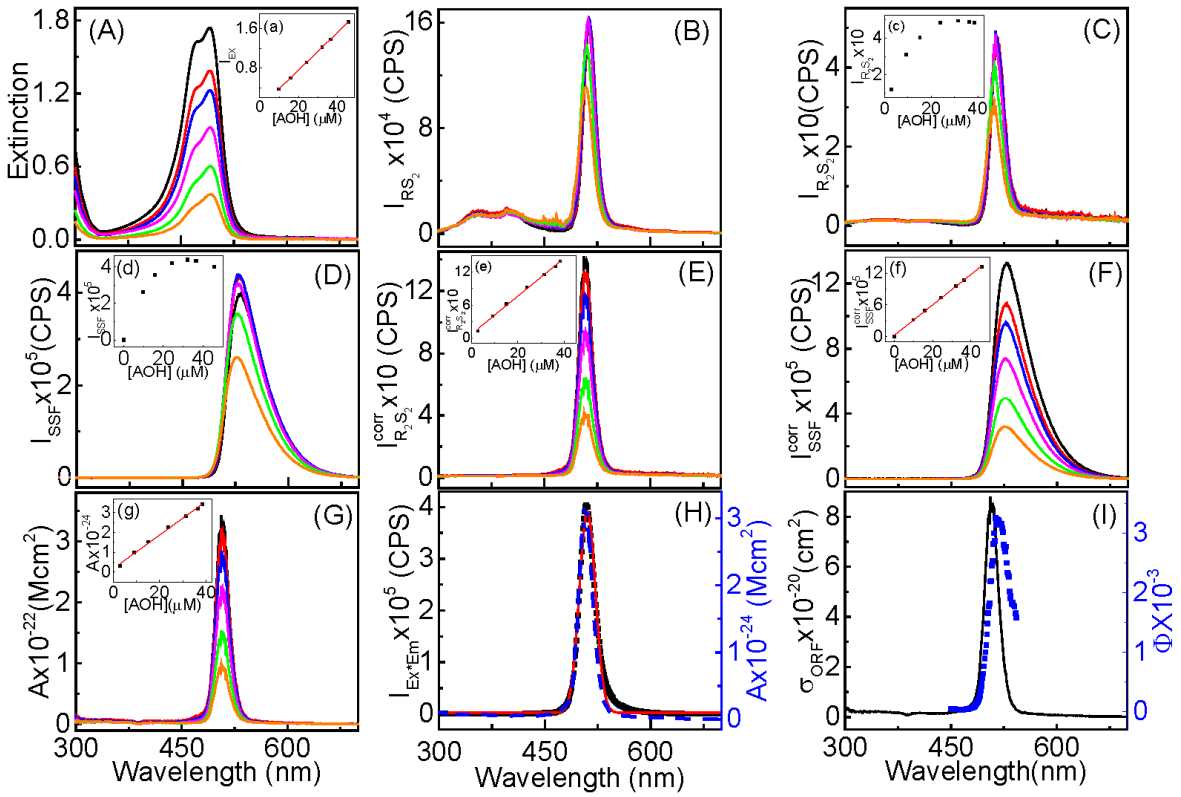

Figure S2. Experimental data obtained with molecular fluorophore AOH. Concentration-dependent (A) fluorophore UV-vis extinction spectra, (B) as-acquired RS_2 spectra, (C) as-acquired R_2S_2 spectra, (D) as-acquired SSF spectra, (E) IFE-corrected R_2S_2 spectra, (F) IFE-corrected SSF spectra, (G) R_2S_2 activity spectra, (H) Comparison of a representative (dash blue line) ORF activity spectrum, (black dots) the multiplication product spectrum of UV-vis excitation and emission spectrum, and the (solid red line) Gaussian curve fitted spectrum. (I) ORF cross-section and quantum yield (blue square) as a function of wavelength. The inset in plots (A), (C), (D), (E), (F), and (G) are spectral peak intensity as AOH concentration.

S5. Experimental data obtained with molecular fluorophore harmane

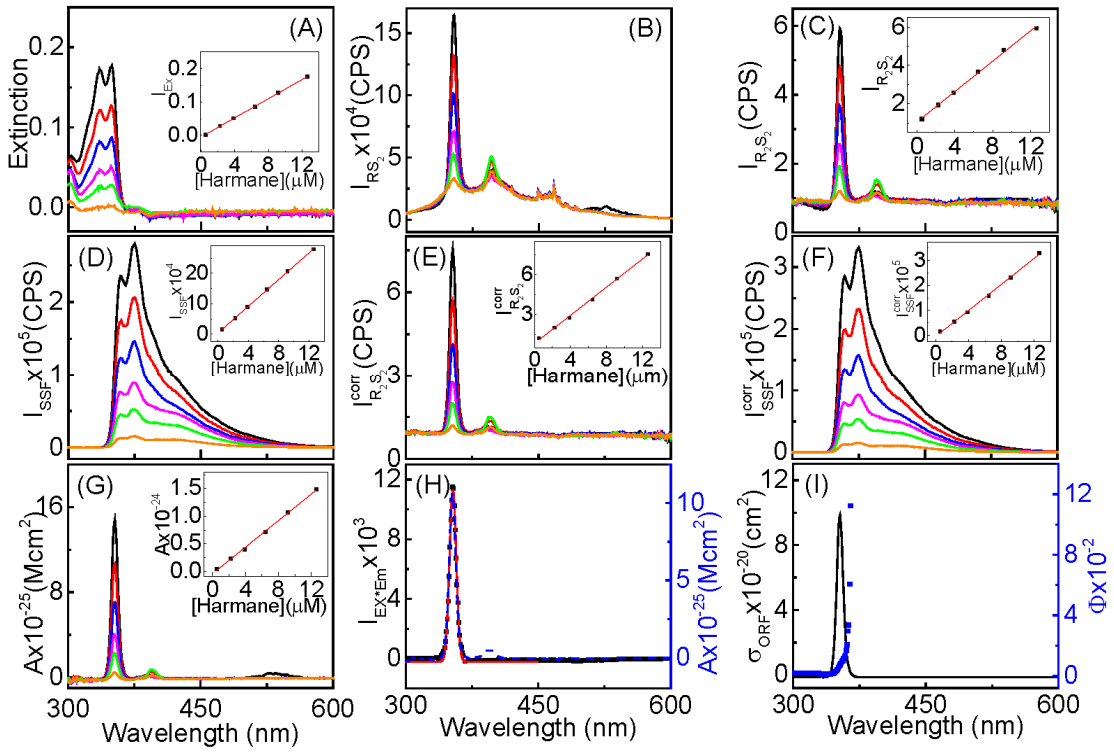

Figure S3. Experimental data obtained with molecular fluorophore harmane. Concentration-dependent (A) fluorophore UV-vis extinction spectra, (B) as-acquired RS_2 spectra, (C) as-acquired R_2S_2 spectra, (D) as-acquired SSF spectra, (E) IFE-corrected R_2S_2 spectra, (F) IFE-corrected SSF spectra, (G) R_2S_2 activity spectra, (H) Comparison of a representative ORF activity spectrum (dash blue line), the multiplication product spectrum (black dots) of UV-vis excitation and emission spectrum, and the Gaussian curve fitted spectrum (solid red line). (I) ORF cross-section and quantum yield (blue square) as a function of wavelength. The inset in plots (A), (C), (D), (E), (F), and (G) are spectral peak intensity as harmane concentration

S6. Experimental data obtained with molecular fluorophore harmine

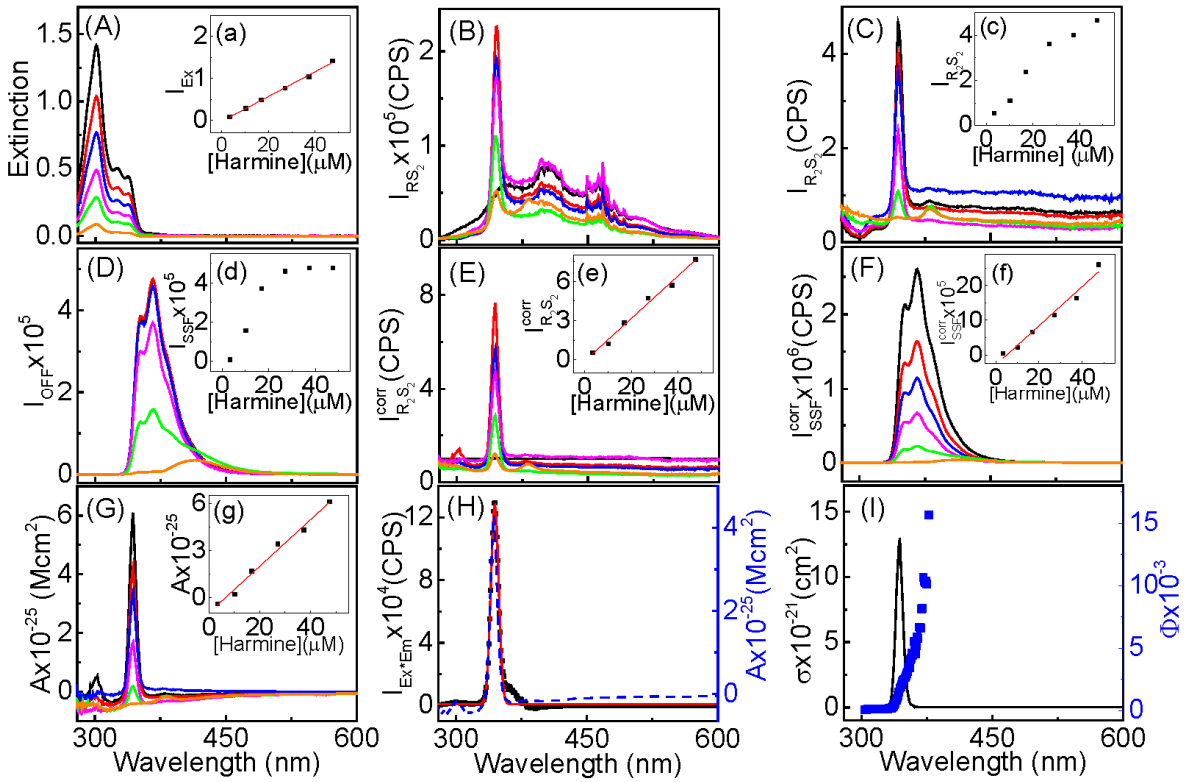

Figure S4. Experimental data obtained with molecular fluorophore harmine. Concentration-dependent (A) fluorophore UV-vis extinction spectra, (B) as-acquired RS_2 spectra, (C) as-acquired R_2S_2 spectra, (D) as-acquired SSF spectra, (E) IFE-corrected R_2S_2 spectra, (F) IFE-corrected SSF spectra, (G) R_2S_2 activity spectra, (H) Comparison of a representative ORF activity spectrum (dash blue line), the multiplication product spectrum (black dots) of UV-vis excitation and emission spectrum, and the Gaussian curve fitted spectrum (solid red line). (I) ORF cross-section and quantum yield (blue square) as a function of wavelength. The inset in plots (A), (C), (D), (E), (F), and (G) are spectral peak intensity as harmine concentration

S7. Experimental data obtained with molecular fluorophore norharmane

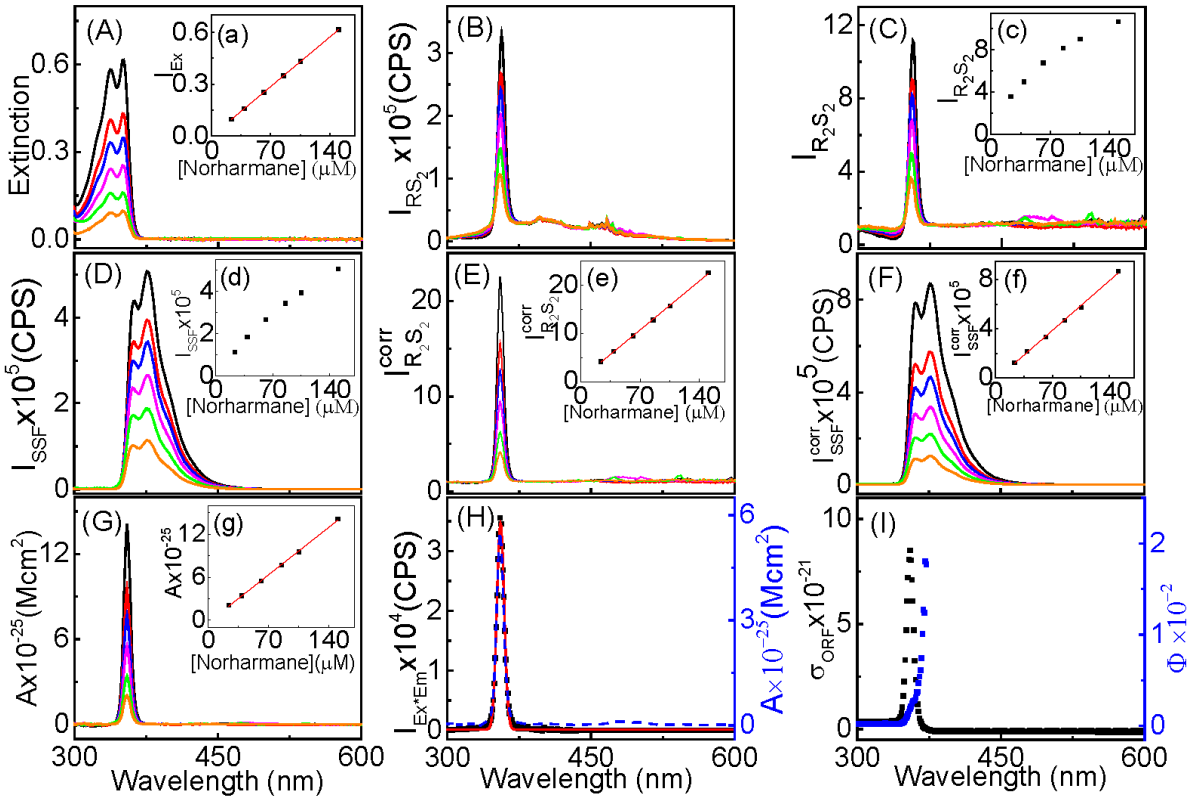

Figure S5. Experimental data obtained with molecular fluorophore norharmane. Concentration-dependent (A) fluorophore UV-vis extinction spectra, (B) as-acquired RS_2 spectra, (C) as-acquired R_2S_2 spectra, (D) as-acquired SSF spectra, (E) IFE-corrected R_2S_2 spectra, (F) IFE-corrected SSF spectra, (G) R_2S_2 activity spectra, (H) Comparison of a representative ORF activity spectrum (dash blue line), the multiplication product spectrum (black dots) of UV-vis excitation and emission spectrum, and the Gaussian curve fitted spectrum (solid red line). (I) ORF cross-section and quantum yield (blue square) as a function of wavelength. The inset in plots (A), (C), (D), (E), (F), and (G) are spectral peak intensity as norharmane concentration

S8. Experimental data obtained with molecular fluorophore zinc phthalocyanine (ZPC)

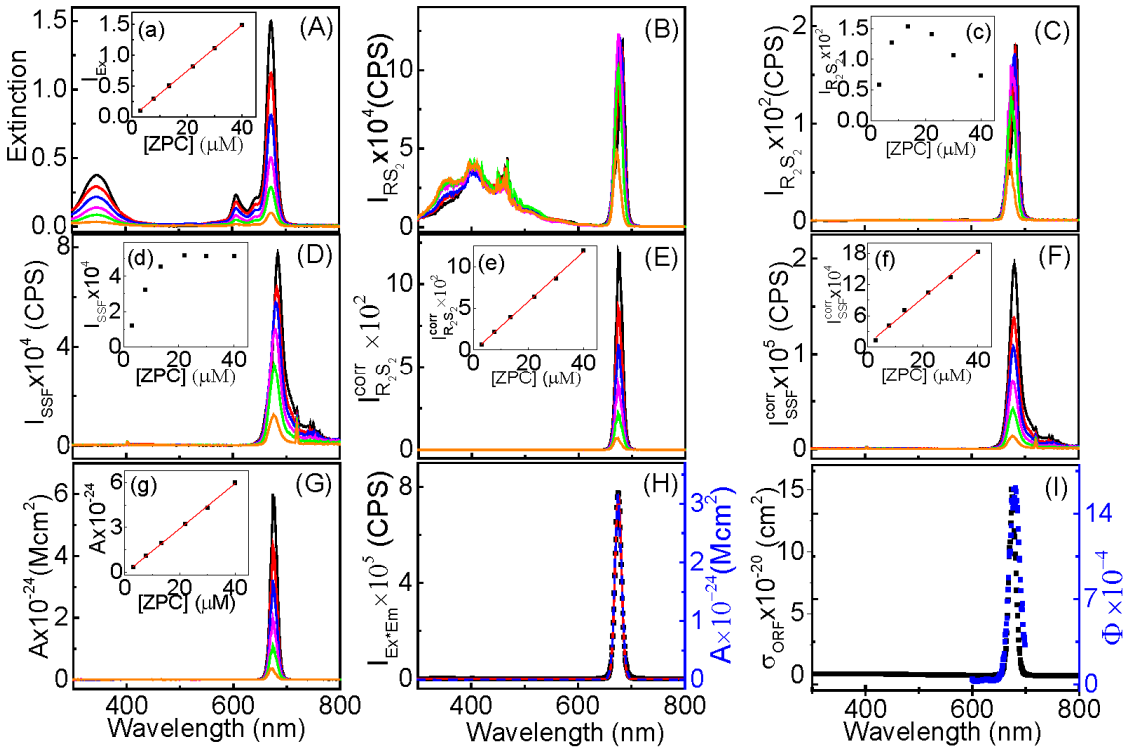

Figure S6. Experimental data obtained with molecular fluorophore ZPC. Concentration-dependent (A) fluorophore UV-vis extinction spectra, (B) as-acquired RS_2 spectra, (C) as-acquired R_2S_2 spectra, (D) as-acquired SSF spectra, (E) IFE-corrected R_2S_2 spectra, (F) IFE-corrected SSF spectra, (G) R_2S_2 activity spectra, (H) Comparison of a representative ORF activity spectrum (dash blue line), the multiplication product spectrum (black dots) of UV-vis excitation and emission spectrum, and the Gaussian curve fitted spectrum (solid red line). (I) ORF cross-section and quantum yield (blue square) as a function of wavelength. The inset in plots (A), (C), (D), (E), (F), and (G) are spectral peak intensity as ZPC concentration

S9. Experimental data obtained with molecular fluorophore cresyl violet perchlorate (CVP)

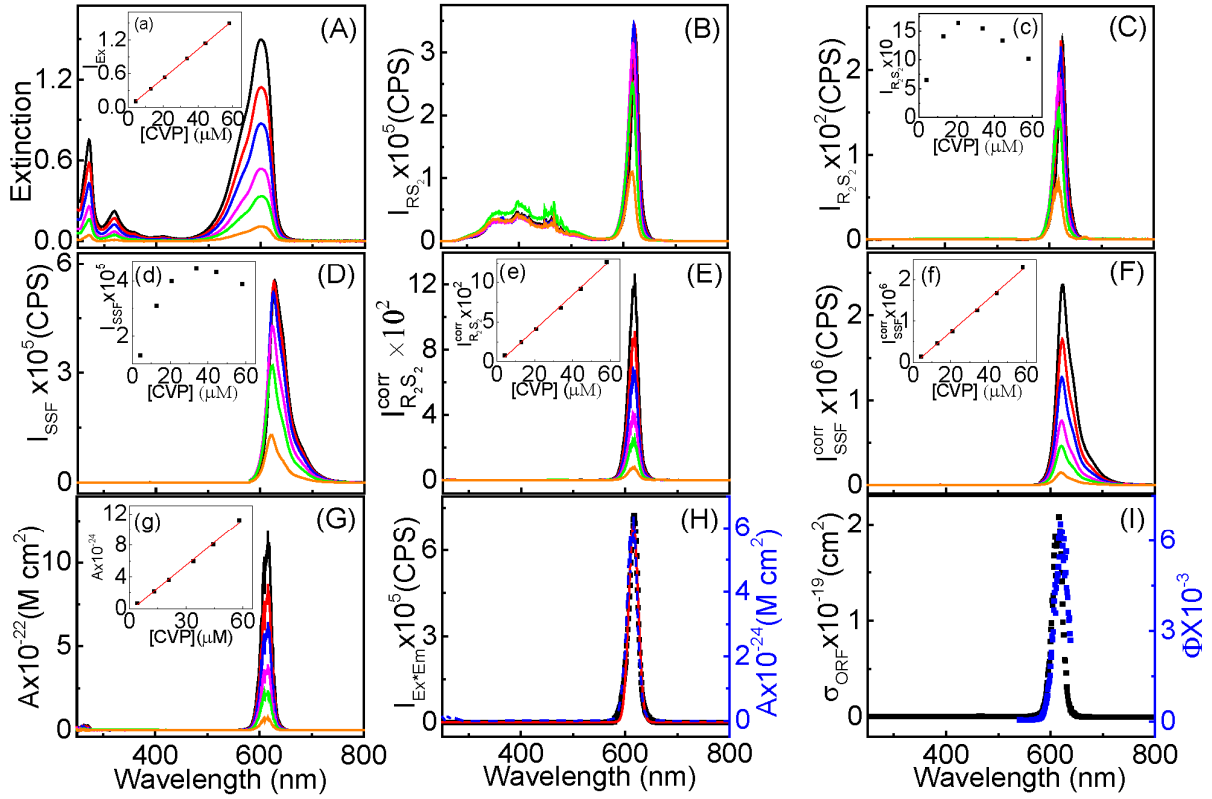

Figure S7. Experimental data obtained with molecular fluorophore CVP. Concentration-dependent (A) fluorophore UV-vis extinction spectra, (B) as-acquired RS_2 spectra, (C) as-acquired R_2S_2 spectra, (D) as-acquired SSF spectra, (E) IFE-corrected R_2S_2 spectra, (F) IFE-corrected SSF spectra, (G) R_2S_2 activity spectra, (H) Comparison of a representative ORF activity spectrum (dash blue line), the multiplication product spectrum (black dots) of UV-vis excitation and emission spectrum, and the Gaussian curve fitted spectrum (solid red line). (I) ORF cross-section and quantum yield (blue square) as a function of wavelength. The inset in plots (A), (C), (D), (E), (F), and (G) are spectral peak intensity as CVP concentration

S10. Experimental data obtained with molecular fluorophore 9,10-Diphenylanthracene (DPA)

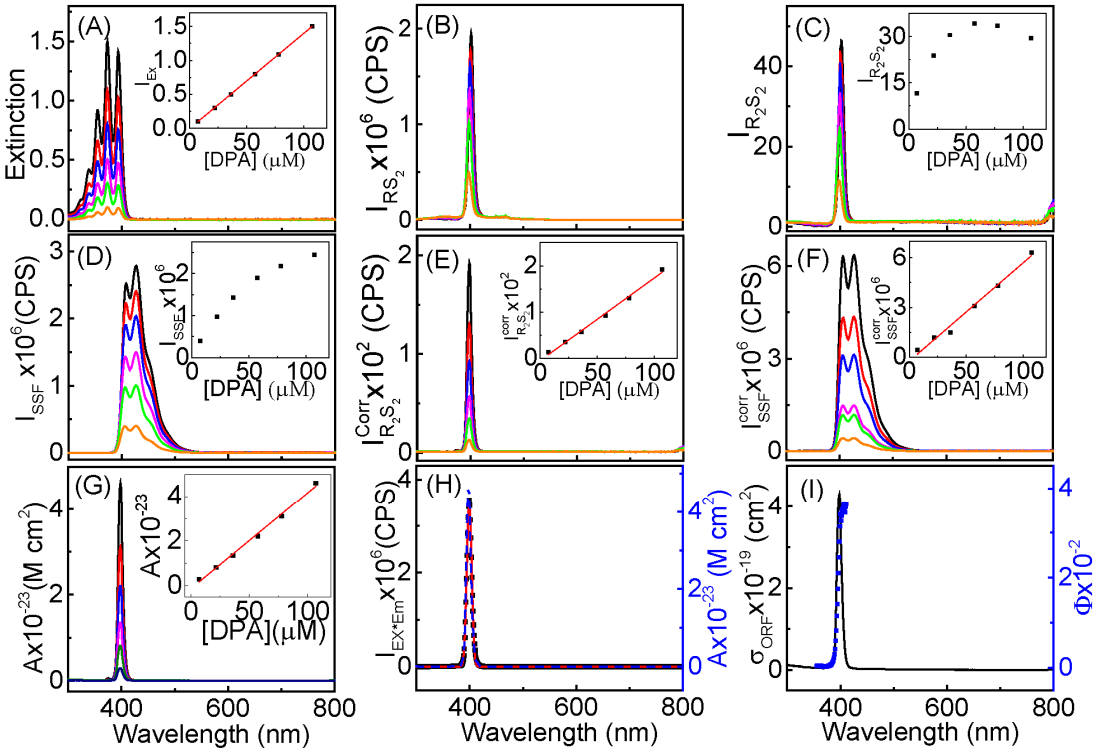

Figure S8. Experimental data obtained with molecular fluorophore DPA. Concentration-dependent (A) fluorophore UV-vis extinction spectra, (B) as-acquired RS_2 spectra, (C) as-acquired R_2S_2 spectra, (D) as-acquired SSF spectra, (E) IFE-corrected R_2S_2 spectra, (F) IFE-corrected SSF spectra, (G) R_2S_2 activity spectra, (H) Comparison of a representative ORF activity spectrum (dash blue line), the multiplication product spectrum (black dots) of UV-vis excitation and emission spectrum, and the Gaussian curve fitted spectrum (solid red line). (I) ORF cross-section and quantum yield (blue square) as a function of wavelength. The inset in plots (A), (C), (D), (E), (F), and (G) are spectral peak intensity as DPA concentration

S11. Experimental data obtained with molecular fluorophore Eosin Y

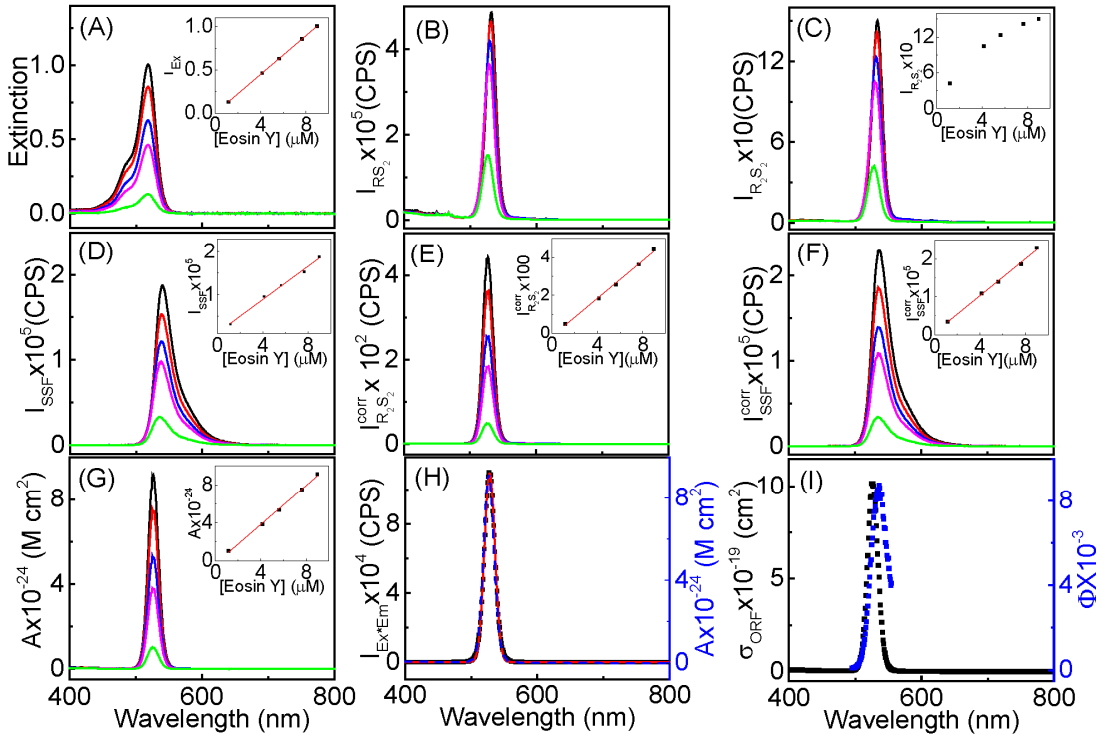

Figure S9. Experimental data obtained with molecular fluorophore Eosin Y. Concentration-dependent (A) fluorophore UV-vis extinction spectra, (B) as-acquired RS_2 spectra, (C) as-acquired R_2S_2 spectra, (D) as-acquired SSF spectra, (E) IFE-corrected R_2S_2 spectra, (F) IFE-corrected SSF spectra, (G) R_2S_2 activity spectra, (H) Comparison of a representative ORF activity spectrum (dash blue line), the multiplication product spectrum (black dots) of UV-vis excitation and emission spectrum, and the Gaussian curve fitted spectrum (solid red line). (I) ORF cross-section and quantum yield (blue square) as a function of wavelength. The inset in plots (A), (C), (D), (E), (F), and (G) are spectral peak intensity as Eosin Y concentration

S12. Experimental data obtained with nanoparticle-fluorophore QD490

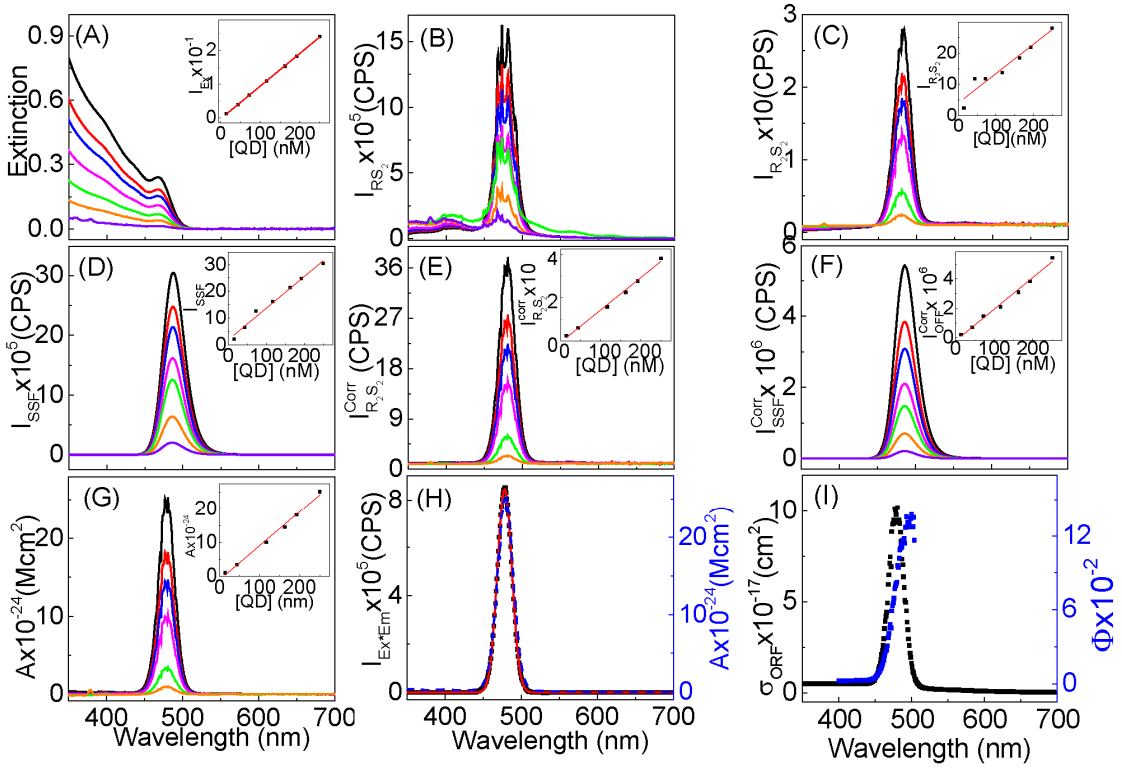

Figure S10. Experimental data obtained with QD490 fluorophore. Concentration-dependent (A) fluorophore UV-vis extinction spectra, (B) as-acquired RS_2 spectra, (C) as-acquired R_2S_2 spectra, (D) as-acquired SSF spectra, (E) IFE-corrected R_2S_2 spectra, (F) IFE-corrected SSF spectra, (G) R_2S_2 activity spectra, (H) comparison of an example ORF activity spectrum, the scaled multiplication product spectrum of UV-vis excitation and emission spectrum, and the Gaussian curve fitted spectrum. (I) ORF cross-section and quantum yield as a function of wavelength. The inset in plots (A), (C), (D), (E), (F), and (G) are spectral peak intensity as QD490 concentration.

S13. Experimental data obtained with nanoparticle-fluorophore QD525

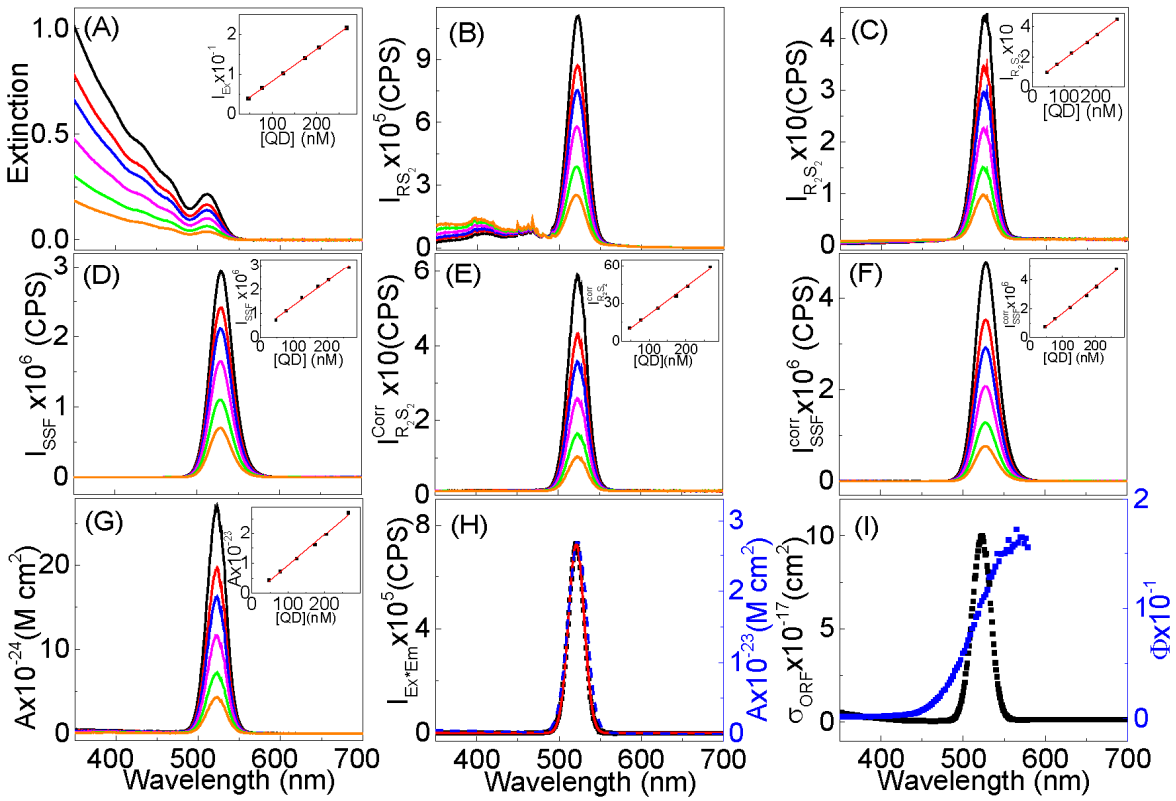

Figure S11. Experimental data obtained with QD525 fluorophore. Concentration-dependent (A) fluorophore UV-vis extinction spectra, (B) as-acquired RS_2 spectra, (C) as-acquired R_2S_2 spectra, (D) as-acquired SSF spectra, (E) IFE-corrected R_2S_2 spectra, (F) IFE-corrected SSF spectra, (G) R_2S_2 activity spectra, (H) comparison of an example ORF activity spectrum, the scaled multiplication product spectrum of UV-vis excitation and emission spectrum, and the Gaussian curve fitted spectrum. (I) ORF cross-section and quantum yield as a function of wavelength. The inset in plots (A), (C), (D), (E), (F), and (G) are spectral peak intensity as QD525 concentration.

S14. Experimental data obtained with nanoparticle-fluorophore QD575

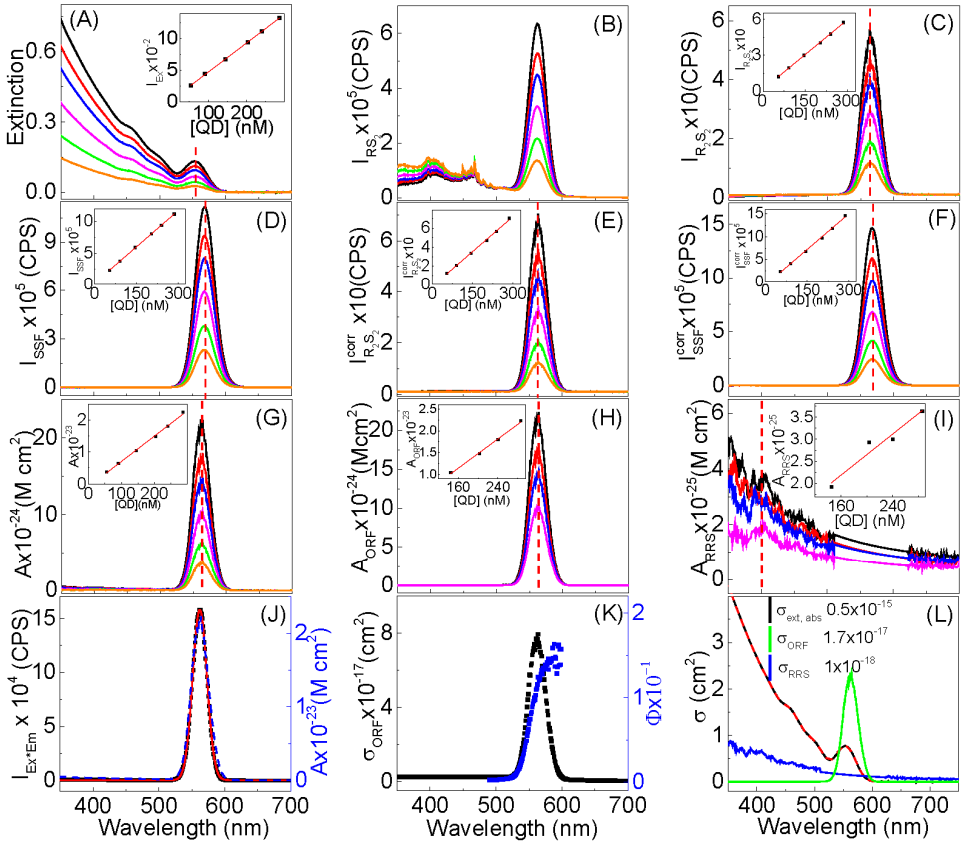

Figure S12. Experimental data obtained with QD575 fluorophore. Concentration-dependent (A) fluorophore UV-vis extinction spectra, (B) as-acquired RS_2 spectra, (C) as-acquired R_2S_2 spectra, (D) as-acquired SSF spectra, (E) IFE-corrected R_2S_2 spectra, (F) IFE-corrected SSF spectra, (G) R_2S_2 activity spectra, (H) ORF activity spectra, (I) RRS activity spectra. The spectral intensities above 550 nm were extrapolated through curve-fitting the measured data from 350 nm to 550 nm using $\sigma_{Sca}=a/\lambda^4$. The insets in (A), (C), (D), (E), (F), (G), (H), and (I) are the spectral peak intensities at the wavelengths shown in red dash line as a function of fluorophore concentration. (J) Comparison of an example (blue dash line) ORF activity spectrum, (black square) the scaled multiplication product spectrum of UV-vis excitation and emission spectrum, and (red solid line) the Gaussian curve fitted spectrum. (K) (black square) ORF cross-section and (blue square) quantum yield as a function of wavelength. (L) The (black) QD575 UV-vis extinction, (red) absorption, (blue) RRS scattering, and (green) on resonance emission cross-section spectrum. The bar in black is the scale for QD UV-vis extinction and absorption cross-sections, the bar in blue and green are for QD the RRS scattering and ORF emission cross-sections, respectively.

S15. Experimental data obtained with nanoparticle-fluorophore QD665

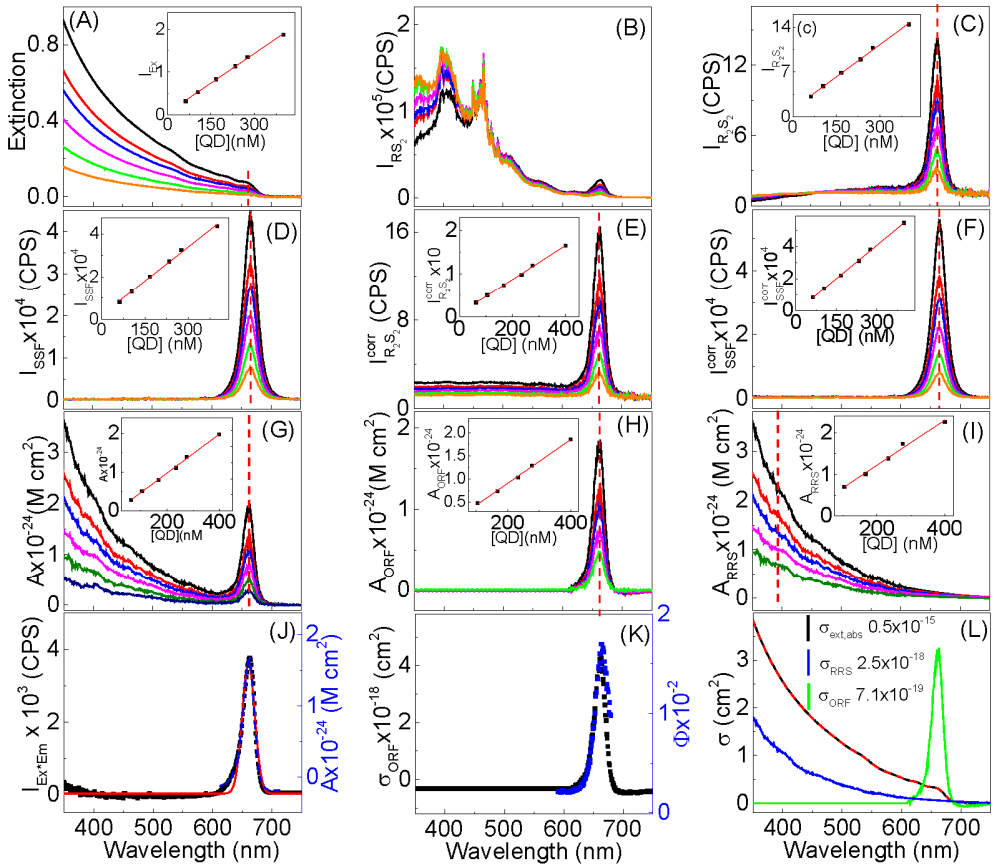

Figure S13. Experimental data obtained with QD665 fluorophore. Concentration-dependent (A) fluorophore UV-vis extinction spectra, (B) as-acquired RS_2 spectra, (C) as-acquired R_2S_2 spectra, (D) as-acquired SSF spectra, (E) IFE-corrected R_2S_2 spectra, (F) IFE-corrected SSF spectra, (G) R_2S_2 activity spectra, (H) ORF activity spectra, (I) RRS activity spectra. The spectral intensities above 550 nm were extrapolated through curve-fitting the measured data from 350 nm to 550 nm using $\sigma_{Sca}=a/\lambda^4$. The insets in (A), (C), (D), (E), (F), (G), (H), and (I) are the spectral peak intensities at the wavelengths shown in red dash line as a function of fluorophore concentration. (J) Comparison of an example (blue dash line) ORF activity spectrum, (black square) the scaled multiplication product spectrum of UV-vis excitation and emission spectrum, and (red solid line) the Gaussian curve fitted spectrum. (K) (black square) ORF cross-section and (blue square) quantum yield as a function of wavelength. (L) The (black) QD665 UV-vis extinction, (red) absorption, (blue) RRS scattering, and (green) on resonance emission cross-section spectrum. The bar in black is the scale for QD UV-vis extinction and absorption cross-sections, the bar in blue and green are for QD the RRS scattering and ORF emission cross-sections, respectively.

S16. Experimental data obtained with nanoparticle-fluorophore QD617

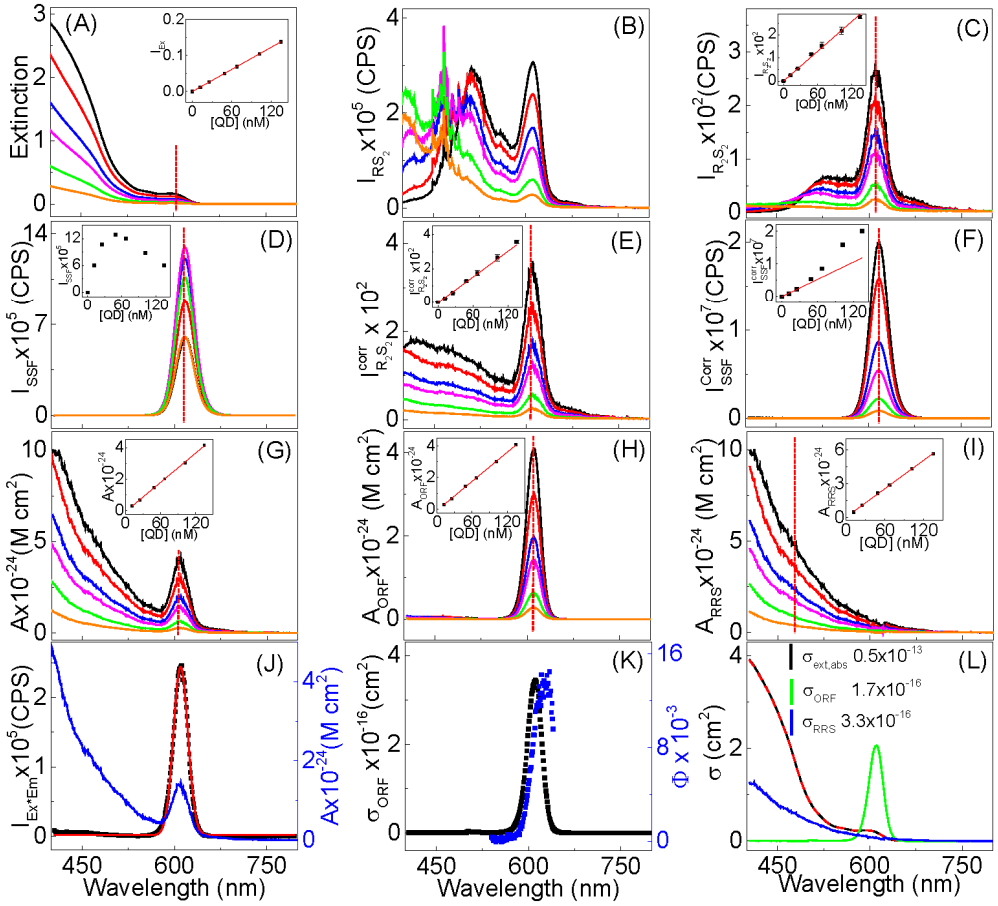

Figure S14. Experimental data obtained with QD617 fluorophore. Concentration-dependent (A) fluorophore UV-vis extinction spectra, (B) as-acquired RS_2 spectra, (C) as-acquired R_2S_2 spectra, (D) as-acquired SSF spectra, (E) IFE-corrected R_2S_2 spectra, (F) IFE-corrected SSF spectra, (G) R_2S_2 activity spectra, (H) ORF activity spectra, (I) RRS activity spectra. The insets in (A), (C), (D), (E), (F), (G), (H), and (I) are the spectral peak intensities at the wavelengths shown in red dash line as a function of fluorophore concentration. (J) Comparison of an example (blue dash line) ORF activity spectrum, (black square) the scaled multiplication product spectrum of UV-vis excitation and emission spectrum, and (red solid line) the Gaussian curve fitted spectrum. (K) (black square) ORF cross-section and (blue square) quantum yield as a function of wavelength. (L) The (black) QD617 UV-vis extinction, (red) absorption, (blue) RRS scattering, and (green) on resonance emission cross-section spectrum. The bar in black is the scale for QD UV-vis extinction and absorption cross-sections, the bar in blue and green are for QD the RRS scattering and ORF emission cross-sections, respectively.

S17. Curve-fitting of the QD RRS cross-sections

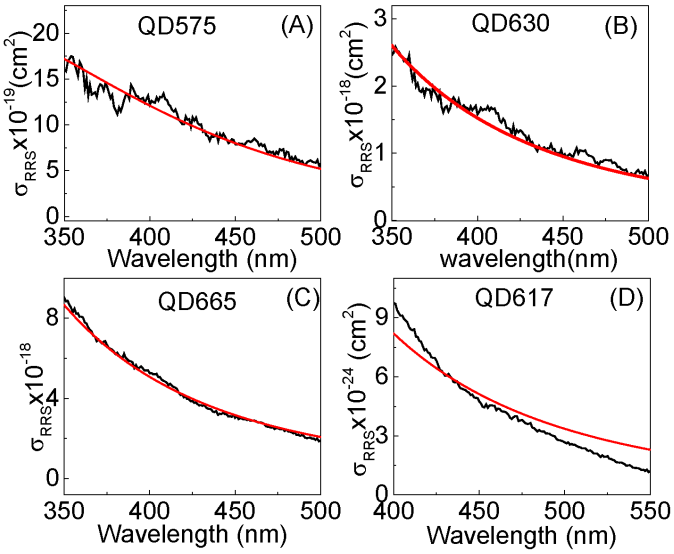

Figure S15. (Black) calculated and (red) fitted RRS cross section (σ_{RRS}) values as a function of wavelength obtained with (A) QD575, (B) QD630, (C) QD665, and (D) QD617. The function for the curve-fitting is $\sigma_{Sca}=a/\lambda^4$. The large derivation between the experimental and fitted RRS cross-sections for QD617 indicates that only can the RRS for QD575, QD630, and QD665 be approximated with the function of $\sigma_{Sca}=a/\lambda^4$ as discussed in the main text.

S18 Determination of wavelength bandwidth of the instrument response peak function

The bandwidth of the instrument response function is related to the slit widths of the excitation and emission monochromators and the wavelength-dependence of the detector response. The bandwidth of the instrument response function was determined by measuring the Rayleigh scattering bandwidth of the 100 nm polystyrene beads by keeping the excitation wavelength at 500 nm but the detection wavelength from 475 nm to 525 nm with wavelength increment of 1 nm. The slit widths of excitation and emission monochromators were both set to be 1 nm, which are the same as that used in the fluorophore SSF and R_2S_2 spectral acquisition. The FWHM of the instrument response is 1.7 nm as shown in Figure S16 through the Gaussian curve-fitting.

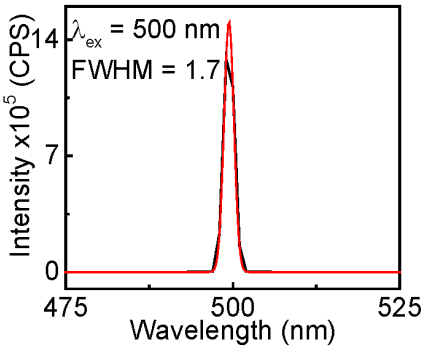

Figure S16. Determination of the bandwidth of the instrument response by measuring the Rayleigh scattering bandwidth of the 100 nm polystyrene beads. The excitation wavelength was kept at 500 nm but the detection wavelength varies from 475 nm to 525 nm with a wavelength increment of 1 nm. The black curve is the experimental data and the red line is obtained by fitting the experimental data with a Gaussian function. The FWHM of the fitting function is 1.7 nm.